ELSEVIER

Surface and Coatings Technology 112 (1999) 15–19

SURFACE & COATINGS TECHNOLOGY

Effects of cusp magnetic field configuration on wave propagation in large diameter r.f. produced plasma

Seiji Takechi *, Shunjiro Shinohara, Yoshinobu Kawai

Interdisciplinary Graduate School of Engineering Sciences, Kyushu University, Kasuga, Fukuoka 816-8580, Japan

Abstract

In order to investigate the effects of cusp magnetic field configuration on r.f. wave propagation, two-dimensional spatial profiles of the excited wave amplitude and phase were measured and were discussed with the spatial distributions of the ion saturation current in a large-diameter plasma. It was shown that in case of the cusp position near the antenna, the excited wave propagated obliquely to the chamber axis, whereas in the case of the position far from the antenna, beyond the position, the traveling wave disappeared. © 1999 Elsevier Science S.A. All rights reserved.

Keywords: Cusp field; Helicon wave; r.f. plasma

1. Introduction

A helicon-wave-produced plasma [1–6] is regarded as one of the candidates for the high-density plasma source required for plasma processing and confinement devices. Various characteristics of the plasma, which is produced by radio frequency (r.f.) waves with the external magnetic field ($\omega_{ci} \ll \omega \ll \omega_{ce}$, where ω_{ci} is the ion cyclotron angular frequency, ω is the driving angular frequency, and ω_{ce} is the electron cyclotron angular frequency), have been investigated in detail experimentally and theoretically. However, most of the results to elucidate the helicon wave physics were undertaken, for simplicity, with the uniform magnetic field.

In the previous work, we demonstrated that a helicon wave with a dominant azimuthal mode number of $m=0$ could be newly excited in a r.f.-produced plasma with a large diameter using a planar, spiral antenna with the uniform magnetic field [7–9]. These results mean that this external magnetic field can be expected to be an additional control parameter for the plasma discharge. Therefore, by changing the various magnetic field configurations, we found that the effective diameter, D_{eff}, defined as the region where the value of the ion saturation current is uniform within $\pm 5\%$ reached ~ 27 cm in the cusp magnetic field configuration [10,11]. Therefore, an analysis of the wave characteristics in the cusp field configuration is very important for produced plasma profiles and also gives us an interesting wave physics, which has been scarcely studied.

In this paper, we present experimentally observed spatial profiles of the excited wave amplitude and phase in a large-diameter r.f.-produced plasma with two cusp magnetic field configurations. The wave propagation characteristics and the comparison with the spatial profiles of the ion saturation current emphasizing the uniformity are also discussed.

2. Experimental

The experimental system was the same as that shown in fig. 1 of Ref. [7]. The four-turn spiral antenna (without Faraday shield) with a diameter of 18 cm was used. Here, $z=0$ cm is defined as being at the window surface that faces an inner vacuum chamber ~ 45 cm in diameter and ~ 170 cm in length. The applied cusp magnetic field was generated by two coils: currents with the same magnitude have opposite directions each other. One case is that the line cusp position, z_{cusp}, was 4 cm, and the central distance, d, between the two coils was 36 cm (Case I). The other case is that $z_{cusp}=30$ cm and $d=42$ cm (Case II). A set containing a contour plot of the magnetic flux and a two-dimensional profile of the

* Corresponding author. Tel: +81 92 5837651;
Fax: +81 92 5718894; e-mail: takechi@aees.kyushu-u.ac.jp

PII S0257-8972(98)00756-7

magnitude of the magnetic field for both two cases are shown in Figs. 1 and 2, respectively.

The r.f. power supply was connected to the antenna through a directional coupler, a matching box and monitors of the antenna voltage and current. Here, the input power was ~300 W, with a frequency of 7 MHz and an Ar filling pressure of 8.5 mTorr in our experiments. The argon plasma parameters were measured by the use of movable and rotatable Langmuir and magnetic probes inserted axially (Case I: the typical measurement region was $z=3\sim50$ cm with $r=0$, 5, 10 and 15 cm; Case II: $z=3\sim66$ cm with $r=0$, 5, 10 and 15 cm, unless specified).

3. Results and discussion

Fig. 3 shows the axial profile of the ion saturation current, I_{is}, for Case I with (a) $I_c=0$ A (b) 30 A, (c) 60 A and (d) 100 A. As I_c increased, in the downstream region, I_{is} was uniform in the r direction. Previous work [10] showed that the effective diameter, D_{eff}, at $z=$ 30 cm reached ~27 cm at $I_c=60$ A, where the electron density $n_e\sim2.5\times10^{11}$ cm^{-3} and electron temperature $T_e\sim2$ eV (radial profile of I_{is} at $z=30$ cm became hollow at $I_c=100$ A, and the D_{eff} became shorter than that at $I_c=60$ A).

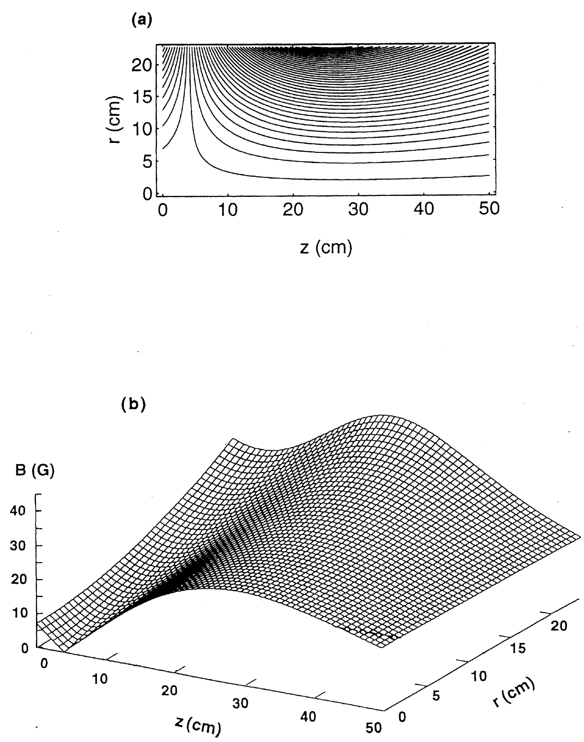

Fig. 1. (a) Contour plot of the magnetic flux. (b) Radial and axial profiles of the magnitude of the external magnetic field. Here, the coil current I_c is 60 A, and the distance d between the two coils is 36 cm (Case I).

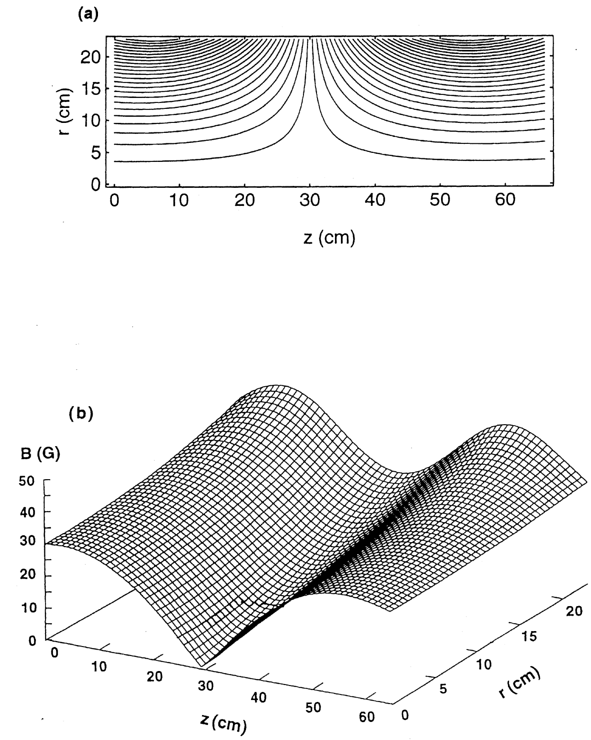

Fig. 2. (a) Contour plot of the magnetic flux. (b) Radial and axial profiles of the magnitude of the external magnetic field. Here, the coil current I_c is 60 A, and the distance d between the two coils is 42 cm (Case II).

Figs. 4 and 5 show contour plots of the amplitude (phase) of B_z (axial component of the excited magnetic fields), in a logarithmic (linear) scale, for Case I with the coil current $I_c=0$, 30, 60 and 100 A. The intervals between the contour lines in Figs. 4 and 5 were 0.2 and $\pi/2$, respectively. In the case of no magnetic field, i.e. Figs. 4(a) and 5(a), the observing region was in a range of $z=3\sim18$ cm, and the amplitude damped strongly with the phase jump near the antenna region [see arrows in Figs. 4(a) and 5(a) at $z\sim4$ cm]. Needless to say, this wave was an evanescent wave in inductively coupled plasma [12], in contrast to a propagating wave, such as a helicon wave. As for the case of $I_c=30$ A [Figs. 4(b) and 5(b)], whose observing (detectable) region was in a range of $z=3\sim21$ cm, the penetration length of the wave was longer, and the z position of the phase jump increased ($z=7$ cm) as compared to those of the case of $I_c=0$ A, but this behavior for $I_c=30$ A was almost similar to that of the evanescent wave.

As for the case of (c) ($I_c=60$ A), the wave damped strongly near the cusp position, and then damped slowly over r–z space after passing through the cusp position. Beyond $z=10$ cm, the phase increased more slowly, i.e. the wave length became longer, but it deviated from the dispersion relation for a helicon wave with uniform plasma [2]. As for the case of (d) ($I_c=100$ A), beyond the cusp position, the amplitude had a tendency to peak

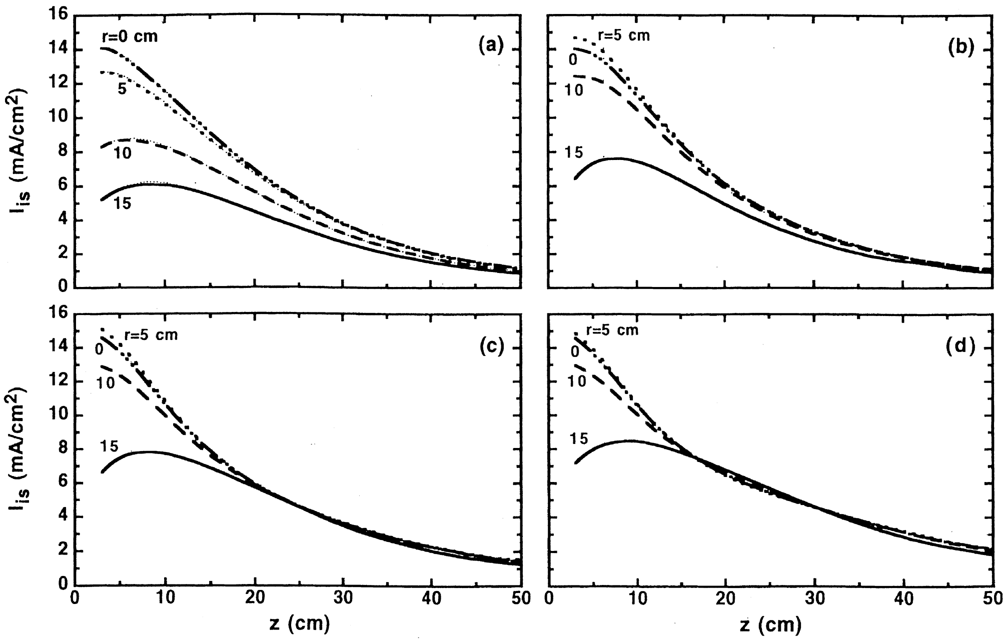

Fig. 3. Axial profiles of ion saturation current I_{is} for Case I with (a) $I_c = 0$ A, (b) 30 A, (c) 60 A and (d) 100 A, respectively.

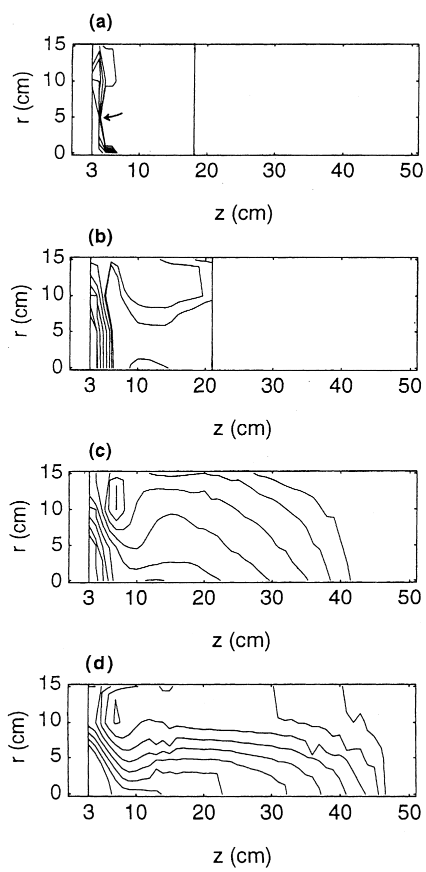

Fig. 4. Contour plot of amplitude in the excited magnetic field B_z for Case I with (a) $I_c = 0$ A, (b) 30 A, (c) 60 A and (d) 100 A.

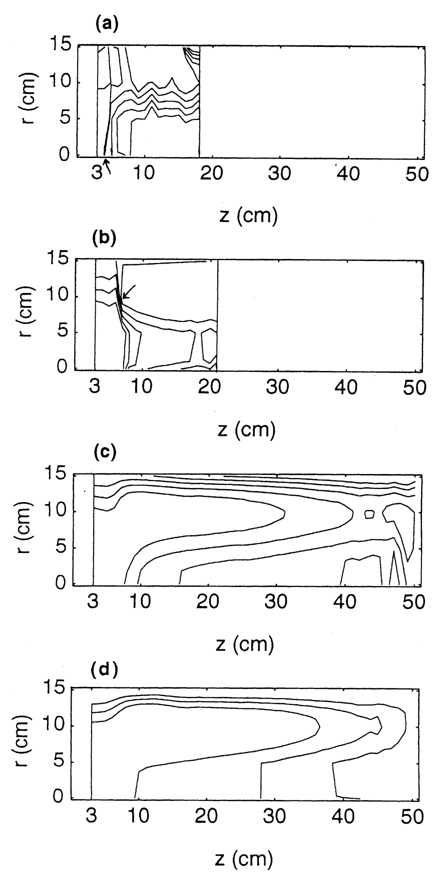

Fig. 5. Contour plot of phase in the excited magnetic field B_z for Case I with (a) $I_c = 0$ A, (b) 30 A, (c) 60 A and (d) 100 A.

in the neighborhood of axis. The excited wave having longer wave length propagated further away from the antenna compared with the case of (c), and the wave length became shorter beyond the coil position ($z=22$ cm). These changes in wavelength, depending on the magnitude of the magnetic field, were consistent with the helicon wave characteristics expected from the helicon wave dispersion relation, but only qualitatively. Therefore, these results indicate that the excited wave propagated obliquely to the chamber axis direction because of the curvature of the magnetic field. Note that as for cases (c) and (d), the wave length at $z<10$ cm with $r=0$ and 5 cm, respectively, satisfied the helicon wave dispersion relation. In the case of (d), there was no traveling wave in the neighborhood of $r=15$ cm.

In the case of $I_c=60$ A, the best uniformity along the radial direction at $z=30$ cm was obtained, and the excited wave, beyond $z=10$ cm, propagated obliquely to the z axis with damping slowly over r–z space. Comparison among these results suggested that it was necessary to obtain a plasma with good uniformity to consider the excited wave propagation region and/or angle with damping length.

Fig. 6 shows an axial profile of the ion saturation current, I_{is}, for Case II with (a) $I_c=0$ A (b) 30 A, (c) 60 A and (d) 80 A. As I_c increased, the peak value of I_{is} shifted to a region further downstream. This result was similar to a previous study [7] with an uniform magnetic field, in which a helicon wave with a $m=0$ mode was excited.

Figs. 7 and 8 show the contour plots of the amplitude (phase) of B_z, in a logarithmic (linear) scale, for Case II with $I_c=0$, 30, 60 and 80 A (in the case of $I_c=30$ A, detectable region was in a range of $z=3\sim38$ cm). The intervals between contour lines in Figs. 7 and 8 were the same as in Figs. 4 and 5, respectively. Note that in the case of $z_{cusp}=36$ cm and $d=100$ cm, the observed radial

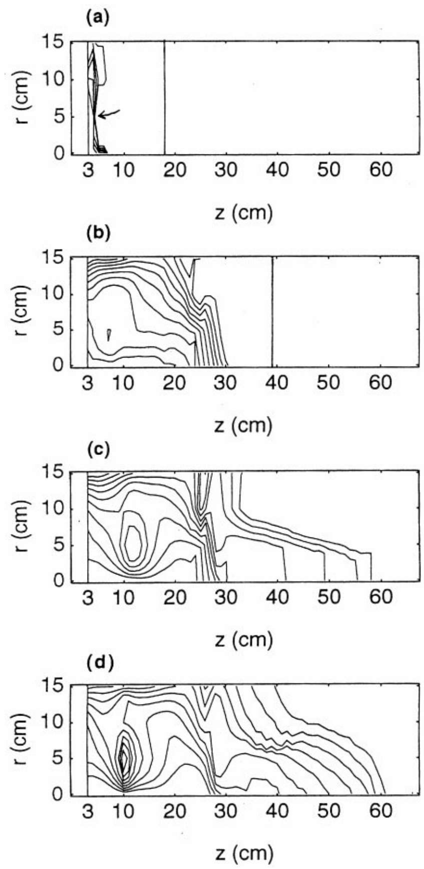

Fig. 7. Contour plot of amplitude in the excited magnetic field B_z for Case II with (a) $I_c=0$ A, (b) 30 A, (c) 60 A and (d) 80 A.

profiles of the excited magnetic fields, at $z=30$ cm, were identical to a helicon wave structure with a dominant azimuthal mode number of $m=0$. As for Case II, the excited wave length at $z<30$ cm satisfied the dispersion relation for a helicon wave. With a further increase in magnetic field with $I_c=30$–80 A, the helicon wave was

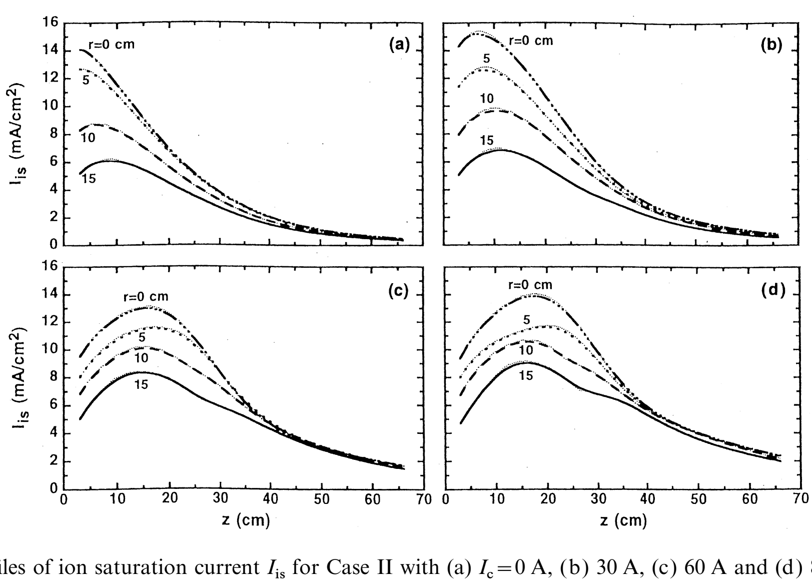

Fig. 6. Axial profiles of ion saturation current I_{is} for Case II with (a) $I_c=0$ A, (b) 30 A, (c) 60 A and (d) 80 A, respectively.

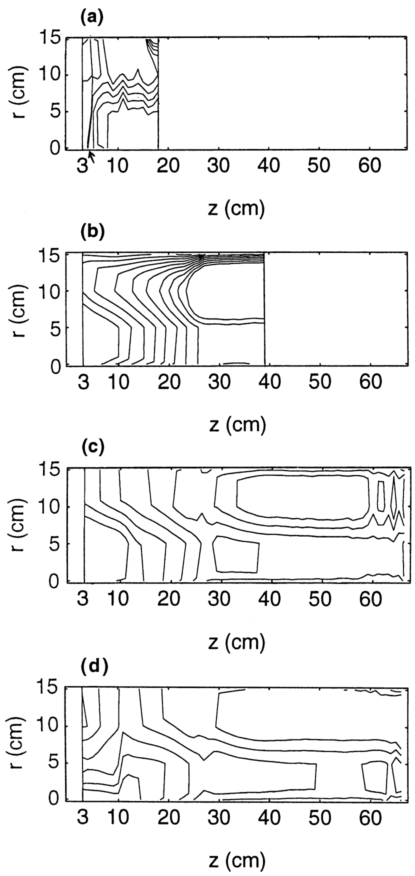

Fig. 8. Contour plot of phase in the excited magnetic field B_z for Case II with (a) $I_c = 0$ A, (b) 30 A, (c) 60 A and (d) 80 A.

excited from any radial position of $r \leqslant 15$ cm ($I_c \geqslant 60$ A), and also the radius of the plasma column became larger, i.e. the wave number perpendicular to the magnetic field lines became smaller from the helicon wave dispersion using the measured electron density and parallel wavelength with the magnetic field strength. This result was consistent with the I_{is} profile: at $z = 3$ cm, the ratio of I_{is} at $r = 0$ cm to that at $r = 15$ cm in the case of (b) was ~ 2.8, whereas the ratio was 1.9 in the cases of (c) and (d). Beyond the cusp position, the wave penetrated further axially with the increase in magnetic field, with no phase change. This showed the existence of a standing wave with a small amplitude ($\sim 10\%$), which is considered to be due to incomplete damping. The plasma discharge could not be maintained above a certain magnitude of the magnetic field ($I_c > 80$ A) due to the poor coupling of the helicon wave with the plasma (measured plasma loading resistance decreased as the magnetic field increased). An unique profile, in which the amplitude decreased strongly and then increased along the axial direction with the large phase change, appeared at $r = 5$ cm and $z = 10$ cm in the case of $I_c = 60$ and 80 A. The behavior can be considered to be partly due to beat wave patterns between the fundamental and the higher-order radial modes [13,14].

4. Conclusions

In order to investigate the effects of the cusp field on r.f. wave propagation, we measured two-dimensional spatial profiles of the excited wave amplitude and the phase with the ion saturation current distributions in the large-diameter (45 cm) r.f.-produced plasma under the two magnetic configurations. As for Case I, i.e. $z_{cusp} = 4$ cm and $d = 36$ cm, the ion saturation current I_{is} was uniform in the r direction, in the downstream region, with an increase in I_c. Only evanescent waves with $I_c \leqslant 30$ A were present, in contrast to a traveling wave with $I_c \geqslant 60$ A. When $I_c = 60$ A, at $z < 10$ cm, the wave first traveled in the z direction initially within a limited region of $r \leqslant 5$ cm, and then propagated obliquely to the z axis in a wide range of r–z space. With a further increase in magnetic field ($I_c > 60$ A), the propagation region became narrow.

As for Case II, i.e. $z_{cusp} = 30$ cm and $d = 42$ cm, as the magnetic field increased, the effective plasma radius became larger, and the helicon wave was excited from any radial position of $r \leqslant 15$ cm from $I_c = 60$ to 80 A. Beyond the cusp position, the standing wave amplitude became larger. It was also shown that the unique behavior, probably due to beat wave patterns between the fundamental and the higher-order radial modes, appeared at $r = 5$ cm and $z = 10$ cm more clearly.

References

[1] R.W. Boswell, Plasma Phys. Control. Fusion 26 (1984) 1147.
[2] F.F. Chen, Plasma Phys. Control. Fusion 33 (1991) 339.
[3] A. Komori, T. Shoji, K. Miyamoto, J. Kawai, Y. Kawai, Phys. Fluids B 3 (1991) 893.
[4] T. Shoji, Y. Sakawa, S. Nakazawa, K. Kadota, T. Sato, Plasma Sources Sci. Technol. 2 (1993) 5.
[5] S. Shinohara, Y. Miyauchi, Y. Kawai, Plasma Phys. Control. Fusion 37 (1995) 1015.
[6] S. Shinohara, Y. Kawai, Jpn. J. Appl. Phys. 34 (1995) L1571.
[7] S. Shinohara, S. Takechi, Y. Kawai, Jpn. J. Appl. Phys. 35 (1996) 4503.
[8] S. Takechi, S. Shinohara, Y. Kawai, Proc. Int. Conf. Plasma Phys. Nagoya, 1996, 10A17.
[9] S. Shinohara, S. Takechi, N. Kaneda, Y. Kawai, Plasma Phys. Control. Fusion 39 (1997) 1479.
[10] S. Takechi, S. Shinohara, Y. Kawai, Jpn. J. Appl. Phys. 36 (1997) 4558.
[11] S. Shinohara, Jpn. J. Appl. Phys. 36 (1997) 4695.
[12] J. Hopwood, Plasma Sources Sci. Technol. 1 (1992) 109.
[13] M. Light, I.D. Sudit, F.F. Chen, D. Arnush, Phys. Plasmas 2 (1995) 4094.
[14] Y. Sakawa, N. Koshikawa, T. Shoji, Plasma Sources Sci. Technol. 6 (1997) 96.